

## Total Hip Prosthesis Metal-Artifact Suppression Using Iterative Deblurring Reconstruction

Douglas D. Robertson, Jie Yuan, Ge Wang, and Michael W. Vannier

---

**Purpose:** CT of total joint prostheses is limited by metal artifact produced mainly by missing projection data. Iterative deblurring reconstruction is less sensitive to missing projection data than filtered backprojection. A software CT simulator was used to compare total hip prosthesis images reconstructed using standard filtered backprojection, filtered backprojection after linear interpolation of missing data, and iterative deblurring.

**Method:** Unilateral and bilateral total hip replacements with metal-backed or all-polyethylene acetabular prostheses were simulated using bone, metal, and polyethylene annuli and circles of metal and water (soft tissue). Material attenuation properties were taken from the literature. The simulation assumed that no X-rays penetrated the metal. Simulated projection data were reconstructed using filtered backprojection, filtered backprojection after linear interpolation of missing data, and iterative deblurring. Visual observations and objective region-of-interest analyses were made.

**Results:** Even with no X-rays penetrating the metal, iterative deblurring produced almost no visible artifact within the bone or soft tissues. Bone edge detection and sizing were more easily and accurately done from the iterative deblurring images. All reconstruction techniques underestimated bone and water CT attenuation values. Metal artifact was worse for the bilateral or metal-backed prostheses.

**Conclusion:** Iterative deblurring generated nearly metal-artifact-free images in this simulation. Filtered backprojection, even after linear interpolation, produced typical clinical metal-artifact images.

**Index Terms:** Computed tomography—Artifact—Computed tomography. reconstruction—Bones, hip—Joints, hip.

---

CT has greatly enhanced the evaluation of the musculoskeletal system. Its cross-sectional and volumetric capabilities provide the potential for thorough and accurate evaluations of the skeleton. Unfortunately, metal artifact severely limits the usefulness of CT for examining bone near total-joint prostheses. Metals, with their higher atomic number and density, attenuate X-rays in the diagnostic energy range much more than do soft tissues or bone. This produces incomplete data or gaps in the respective portions of the CT projection data (1–3). Image reconstruction using filtered backprojection produces star-burst artifacts (streaking) in the processed images. These artifacts seriously degrade image quality, particularly near the surface of the metal object.

Metal artifact has been reduced or suppressed by (a) scanning objects made from less-attenuating materials and made with small cross sections (3–5), (b) increasing the effective energy of the X-ray beam (4,5), (c) generating values for the incomplete projection data (1,2,5–8), and (d) using different reconstruction mathematics that are less sensitive to incomplete data (9,10). Methods a and b are limited by the materials from which prostheses are made, the sizes in which they are made, permissible patient dosing, and by the fact that optimal bone mineral detection requires low effective energies (11). Method c involves artificially generating values for the missing data in the raw data and reconstructing the new data set with standard reconstruction algorithms. The exact values given to the projection gaps are not critical, and several techniques have been used to automatically create the missing data (1,2,5–8). One method, implemented by Kalender and Hebel (2) and used in this study, uses linear interpolation of the adjacent raw data that is not affected by the metal to fill in the gaps. Standard filtered backprojection is then used to reconstruct a new image.

---

From the Mallinckrodt Institute of Radiology (D. D. Robertson, J. Yuan, G. Wang, and M. W. Vannier), and the Department of Orthopaedic Surgery (D. D. Robertson), Washington University School of Medicine, St. Louis, MO, U.S.A. Address correspondence and reprint requests to Dr. D. D. Robertson at Mallinckrodt Institute of Radiology, 510 South Kingshighway Boulevard, St. Louis, MO 63110, U.S.A.

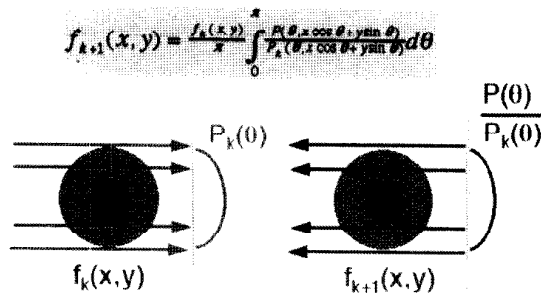


**FIG. 1.** Iterative deblurring reconstruction. Projection (left)/ Backprojection (right). This formula is used to reconstruct straight ray tomography when metal is not present. The projection profile is  $P(\theta, t) = \int_{-R}^R \int_{-R}^R f(x, y) \delta(x \cos \theta + y \sin \theta - t) dx dy$ ,  $\theta \in [0, \pi]$ ,  $t \in [-R, R]$ .

Currently, only investigational implementations are installed.

Iterative reconstruction algorithms, with and without incorporation of a priori information, have been used to reconstruct incomplete projections (9,10). Although previous results using iterative reconstruction were unsatisfactory, a recently developed iterative deblurring method has produced image reconstructions of incomplete data with little artifact (12). This iterative method has been used in various other applications (13–16).

From a theoretical viewpoint, iterative reconstruction has the potential to produce optimal results given a set of incomplete projection data (Fig. 1). Iterative reconstruction involves initially making a guess, typically a constant, about the appearance of the image. Current guesses in each iteration are then projected along the X-ray paths to obtain estimated projection profiles. Every physically measured projection profile is then divided point by point by the estimated counterpart. The ratio profiles are then backprojected onto the field of view. Finally, the backprojected image is multiplied point by point by the current guess image to produce a better guess. When metal is present, the integral region is restricted to the

nonmetal area and the denominator  $p$  (illustrated in Fig. 1) is replaced by a function of  $x, y$ . All iterative calculations will improve the result, i.e., convergence is guaranteed (9,10).

A software CT simulator was used to compare total hip prosthesis images reconstructed using standard filtered backprojection, filtered backprojection after linear interpolation of missing data, and iterative deblurring.

**MATERIALS AND METHODS**

The process used to accomplish this study is diagrammed in the flowchart (Fig. 2). Four different non-cemented total hip replacements were mathematically modeled using annuli of bone (acetabulum), metal (acetabular prosthesis), polyethylene (acetabular prosthesis), and circles of metal (femoral prosthesis head) and water (soft tissue). Two models were made of a unilateral prosthesis, one with a metal-backed acetabular prosthesis and one with an all-polyethylene acetabular prosthesis (Fig. 3). The  $256 \times 256$ -pixel model had a field of view of 120 mm. Two models were made of bilateral prostheses, one with bilateral metal-backed acetabular prostheses and one with bilateral all-polyethylene acetabular prostheses (Fig. 4). The  $256 \times 256$ -pixel model had a field of view of 284 mm. Bone, polyethylene, and water were assigned CT values of 1,000, 0, and  $-40$  Hounsfield units, respectively. These values are representative of attenuation properties described in the literature (17,18).

A previously described (12) software CT simulator was used to perform standard filtered backprojection, an implementation of filtered backprojection after linear interpolation as described by Kalender and Hebel (2), and iterative deblurring. A point source and point detectors were assumed. Reconstruction was performed using 256 parallel-beam projections, 256 detectors per projection, and  $180^\circ$  scanning. The software was written in C and simulations were run on a Sparc 10 (Sun Microsystems, Inc., Mountain View, CA, U.S.A.).

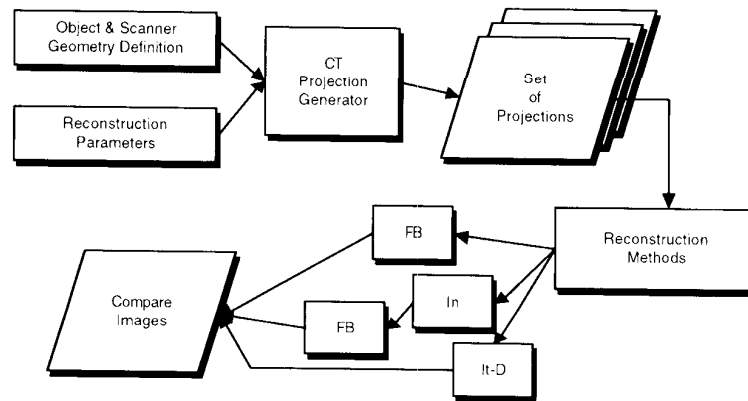


**FIG. 2.** Flowchart for the comparison of total hip prosthesis images reconstructed using standard filtered backprojection, filtered backprojection after linear interpolation of missing data, and iterative deblurring. FB, filtered backprojection; In, interpolation of missing projection data; It-D, iterative deblurring.

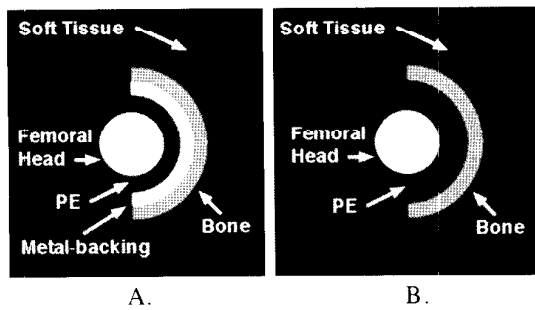


**FIG. 3.** Unilateral total hip replacement model. **A:** Metal-backed acetabular prosthesis. **B:** All-polyethylene acetabular prosthesis. PE, polyethylene.

The simulation assumed the practical but extreme condition in which no X-rays penetrate the metal. Projection masks were produced by projecting a mask of the location of the metal within the field of view along the various directions and setting the value to 0 or 1. Projection ray values were calculated along paths where the projection mask had only zeros (no metal within that projection). Projection ray values were not calculated along paths where the projection mask had a 1 within it (metal within that projection).

Iterative deblurring images were reconstructed with 80 iterations. The initial guess was selected to be an image whose matrix had the same constant value. For each iteration, projection and backprojection were performed only if the interpolation involved no pixels in the metal mask and no detectors were blocked by the projection mask. The method of filtered backprojection after linear interpolation of missing data was implemented by identifying projection gaps directly from the projection mask. The missing data were then linearly filled in using the two nearest neighboring detectable projection values.

All reconstructed images were visually assessed for the presence of metal artifact. The accuracy of the cortical bone edges was assessed using ANALYZE™ (19) to measure thickness at the midpoint of the bone annuli. These measurements were compared with the known cortical thickness of the model (7 mm). The amount of artifact within bone and water was objectively measured. ANALYZE™ (18) was used to calculate average and standard deviation values for regions of interest for the bone annulus, all water within the image, and a  $142 \times$

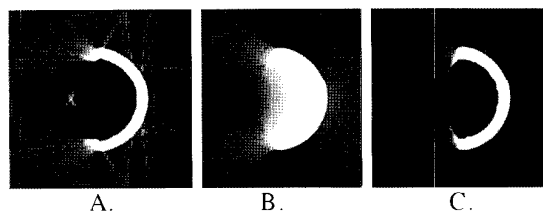


**FIG. 5.** Metal-backed acetabular prosthesis unilateral total hip replacement. **A:** Standard filtered backprojection. **B:** Filtered backprojection after linear interpolation. **C:** Iterative deblurring.

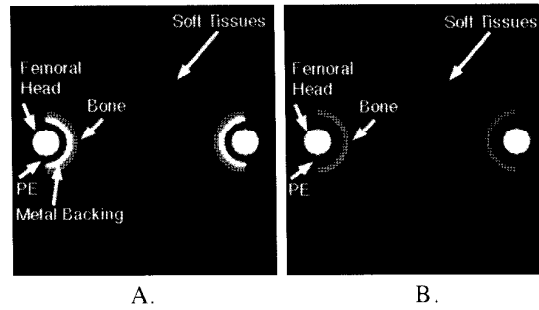


**FIG. 4.** Bilateral total hip replacement model. **A:** Metal-backed acetabular prosthesis. **B:** All-polyethylene acetabular prosthesis. PE, polyethylene.

68-mm rectangle of water centered between the bilateral prostheses.

## RESULTS

Figures 5–8 illustrate the images produced using the three reconstruction techniques. The area between the prosthetic femoral head and the metal-backed acetabulum is void of information because no X-rays reach this area in the simulation. Note the moderate to severe artifact in the soft tissue, especially in between the bilateral prostheses, and adjacent to bone regions in the images produced by filtered backprojection, with and without linear interpolation of missing data. Iterative deblurring reconstruction reduces this artifact. Visually the artifact within water appears worse with a metal-backed acetabular prosthesis compared with the all-polyethylene acetabular prosthesis and with the bilateral prostheses compared with the unilateral prosthesis.

Bone edges were easier to detect on the images generated using iterative deblurring and filtered backprojection. As depicted in Fig. 5 and 7, bone edges produced by filtered backprojection after linear interpolation were blurred. The cortical bone thickness measurements, at the midpoint of the bone annulus, were most accurate for the iterative deblurring images (Table 1). All-polyethylene prostheses produced more accurate cortical thickness measurements than the metal-backed prostheses.

CT attenuation values within the bone annuli and wa-

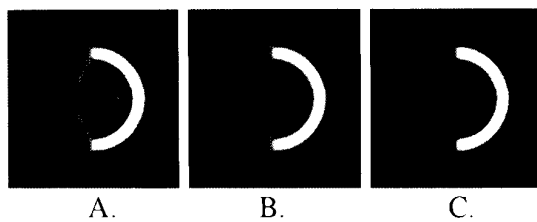


**FIG. 6.** All-polyethylene acetabular prosthesis unilateral total hip replacement. **A:** Standard filtered backprojection. **B:** Filtered backprojection after linear interpolation. **C:** Iterative deblurring.

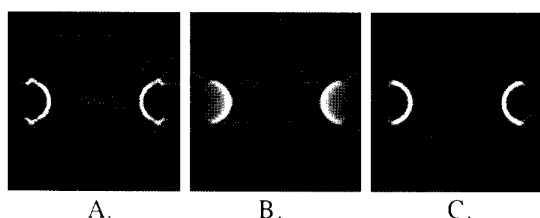


**FIG. 7.** Metal-backed acetabular prosthesis bilateral total hip replacement. **A:** Standard filtered backprojection. **B:** Filtered backprojection after linear interpolation. **C:** Iterative deblurring.

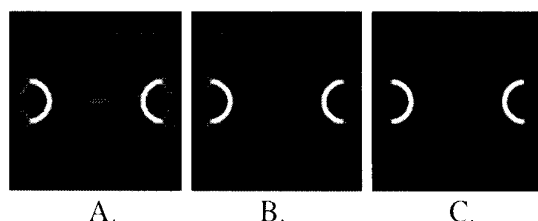


**FIG. 8.** All-polyethylene acetabular prosthesis unilateral total hip replacement. **A:** Standard filtered backprojection. **B:** Filtered backprojection after linear interpolation. **C:** Iterative deblurring.

ter regions of interest were less than the values of the model (Tables 2 and 3). All three reconstruction techniques decreased the values compared with the model values. With respect to the bone values, this effect was less for the iterative deblurring images, the unilateral prosthesis, and the all-polyethylene acetabular prostheses.

Objective analysis corroborated our subjective findings. Iterative deblurring produced the lowest standard deviations (reflecting less noise and artifact) for the water values (Tables 2 and 3). This was true when the region of interest included all the water values within the image, and it was especially true when the water between the bilateral prostheses was examined.

## DISCUSSION AND CONCLUSION

Experimental and clinical examples of the nearly artifact-free images have been obtained with prostheses made from the less dense and lower effective atomic number titanium 6/4 alloy (4,5) and small pieces of more highly attenuating alloys, such as cobalt-chrome (3,4). Although technique can be adjusted to improve CT images, flexibility is limited by several factors: patient dose; the requirement of a low effective energy for optimal bone mineral detection (11); the selection of prosthesis not being based on attenuation coefficients; and prosthesis size being determined by the patient. Thus, metal artifacts will occur, and other techniques are needed to suppress them.

The artifacts in the images produced by filtered back-

projection and filtered backprojection after linear interpolation were realistic and resembled actual patient images. The more metal present in the field of view (metal backed and bilateral prostheses), the more the metal artifact that was produced. Reconstruction of the incomplete projection data using iterative deblurring produced an essentially metal-artifact-free image for bone and soft tissues and had performance that was superior to the filtered backprojection methods. These results were obtained with the extreme condition in which no X-rays penetrated any metal. This was extreme because as already noted, X-rays can pass through moderately thick pieces of titanium alloy and small pieces of cobalt chrome alloy to produce nearly artifact-free images.

Bone edges were more easily found and thickness measurements were more accurately made in the iterative deblurring images. The filtered backprojection images sometimes had streaks in the regions where the measurement was made, decreasing the certainty of the edge's location. Filtered backprojection blurred the edges and attempted to fill in the missing information in the region of the metal, decreasing edge selection certainty. Bone edges in the iterative deblurring images were relatively crisp, far less ambiguous, and thus easier to detect and measure.

Iterative deblurring was more computationally costly, requiring approximately a twofold increase in the cpu time to reconstruct an image compared with filtered backprojection with or without linear interpolation. It also would be not as computationally efficient as the

**TABLE 1.** Cortical bone thickness measurements<sup>a</sup>

	FB (mm)	FB-In (mm)	It-D (mm)
Unilateral			
Metal backed	6.5	6.2	6.8
All polyethylene	6.8	6.8	7
Bilateral <sup>b</sup>			
Metal backed	6.2	6.2	7
All polyethylene	6.6	6.6	7

FB, filtered backprojection; FB-In, filtered backprojection after linear interpolation; It-D, iterative deblurring.

<sup>a</sup> Model cortical thickness was 7.0 mm.

<sup>b</sup> Prosthesis on left side of image measured.

**TABLE 2.** Unilateral total hip prosthesis simulation

	Bone	Water
Metal backed		
Model	1,000 ± 0	0 ± 0
FB	748 ± 254	-25 ± 75
FB-In	789 ± 125	-19 ± 46
It-D	824 ± 216	-25 ± 28
All polyethylene		
Model	1,000 ± 0	0 ± 0
FB	814 ± 55	-24 ± 34
FB-In	820 ± 50	-26 ± 26
It-D	830 ± 66	-25 ± 16

Values represent the average ± SD pixel values for the bone and water annuli. FB, filtered backprojection; FB In, filtered backprojection after linear interpolation; It-D, iterative deblurring.

TABLE 3. Bilateral total hip prosthesis simulation

	Bone R	Bone L	Water total	Water center
Metal backed				
Model	1,000 ± 0	1,000 ± 0	0 ± 0	0 ± 0
FB	638 ± 370	648 ± 358	-22 ± 74	-27 ± 71
FB-In	720 ± 153	727 ± 154	-24 ± 32	-36 ± 46
It-D	832 ± 283	821 ± 237	-25 ± 18	-24 ± 6
All polyethylene				
Model	1,000 ± 0	1,000 ± 0	0 ± 0	0 ± 0
FB	787 ± 114	782 ± 119	-24 ± 52	-27 ± 66
FB-In	794 ± 73	794 ± 71	-26 ± 23	-29 ± 23
It-D	841 ± 60	841 ± 59	-25 ± 14	-28 ± 7

Values represent the average ± SD pixel values for the bone (right and left annuli) and water. The water values were calculated for all the water within the image (total) and for a rectangular region of interest between the two prostheses (center). FB, filtered backprojection; FB-In, filtered backprojection after linear interpolation; It-D, iterative deblurring.

pattern recognition method of Morin and Raesides (7). However, iterative deblurring produced superior images compared with filtered backprojection. It is also not limited in cases in which the metal blocks portions of the central projection—cases that the pattern recognition method (7) would be unable to generate missing values for.

Unlike clinical CT systems, all reconstructions in this study were performed without hardware acceleration. In investigational studies, lack of hardware acceleration should not be a limitation. However, for routine clinical studies, the computational time could be a limitation. This could be overcome by designing dedicated hardware or using parallel computing to perform portions of the iterative deblurring reconstruction.

In this study, iterative deblurring was stopped at 80 iterations. Fewer iterations would reduce the computational time. However, although convergence is guaranteed (9,10), the elucidation of an optimal stopping criterion is not. Visual assessments can be made and no further iterations made when no new improvement in the image quality is detected. Twenty and 80 iterations were tried in this study and we thought that 80 iterations improved the visual quality of the images. Discrepancy curves (between iterations) of the projection profiles may be plotted and the iterations stopped when the curves become flat (i.e., little difference between two iterations). Work is under way to implement this objective method for determining the stopping criterion.

Reducing metal artifact from hip prostheses is important. Reduced metal artifact in the soft tissues adjacent to prostheses, such as the pelvic sidewall, will improve our assessments of post-traumatic or postoperative complications, tumor response or recurrence, and nonrelated diseases and conditions. Clearer and more accurate bone edges near prostheses will permit improved assessments of the bone's response to the prosthesis and of the remaining bone before revision surgery.

In conclusion, iterative deblurring was far less sensitive to missing projection data, producing nearly metal-artifact-free images of simulated unilateral and bilateral

total hip prostheses. For difficult cases, iterative deblurring seems to be a potential solution for severe metal artifact. More comparison between our method and others, including the method of Morin and Raesides (7), will be performed. Work continues to bring this investigational process to clinical use.

**Acknowledgment:** We acknowledge B. Brunsten's and R. Walkup's technical support. The ANALYZE™ software system from Dr. Richard A. Robb and associates at the Mayo Biomedical Imaging Resource was used in this study.

## REFERENCES

- Hinderling T, Ruegsegger P, Anliker M, Dietschi C. Computer tomography reconstruction from hollow projections: An application to in vivo evaluation of artificial hip joints. *J Comput Assist Tomogr* 1979;3:52-7.
- Kalender WA, Hebel R. Fast routine for reduction of artifacts caused by metallic implants in CT images. *Radiology* 1986;161:345.
- Robertson DD, Magid D, Poss R, Fishman EK, Brooker AF, Sledge CB. Enhanced computed tomographic techniques for the evaluation of total hip arthroplasty. *J Arthroplasty* 1989;4:271-6.
- Robertson DD, Weiss P, Fishman EK, Magid D, Walker PS. Evaluation of CT techniques for reducing artifact in the presence of metallic orthopedic implants. *J Comput Assist Tomogr* 1988;12:236-41.
- Seitz P, Ruegsegger P. CT bone densitometry of the anchorage of artificial knee joints. *J Comput Assist Tomogr* 1985;9:612-22.
- Lewitt RM, Bates R. Image reconstructions from projections: II. Projection completion methods. *Optik* 1978;50:189-204.
- Morin RL, Raesides D. A pattern recognition method for the removal of streaking artifact in computed tomography. *Radiology* 1981;141:229-33.
- Seitz P, Ruegsegger P. Anchorage of femoral implants visualized by modified computed tomography. *Arch Orthop Trauma Surg* 1982;100:261-6.
- Csiszar I. Why least squares and maximum entropy? An axiomatic approach to inference for linear inverse problems. *Ann Statistics* 1991;19:2032-66.
- Snyder DL, Schultz T, O'Sullivan J. Deblurring subject to non-negativity constraints. *IEEE Trans Signal Proc* 1992;40:1143-50.
- Muller A, Ruegsegger P. Optimal settings for the evaluation of perimenopausal bone loss. *J Comput Assist Tomogr* 1985;9:607-8.
- Wang G, Snyder D, O'Sullivan J, Vannier M. Iterative deblurring

- for CT metal artifact reduction. *IEEE Trans Med Imaging* 1996;15:657-64.
13. Holmes TM. Maximum-likelihood image restoration adapted for noncoherent optical imaging. *J Opt Soc Am* 1988;5:666-73.
  14. Lucy L. An iterative technique for the rectification of onservred distributions. *Astronom* 1974;79:745-54.
  15. Richardson WH. Bayesian-based iterative method of image restoration. *J Opt Soc Am* 1972;162:55-9.
  16. Shepp LA, Vardi Y. Maximum likelihood reconstruction for emission tomography. *IEEE Trans Med Imaging* 1982;MI-1:113-21.
  17. White DR. Tissue substitutes in experimental radiation physics. *Med Phys* 1978;5:467-79.
  18. Steenbeek JC, van Kuijk C, Grashuis JL. Influence of calibration materials in single- and dual-energy quantitative CT. *Radiology* 1992;183:849-55.
  19. Robb RA. *ANALYZE<sup>TM</sup> reference manual*, 7th ed. Biomedical Imaging Resource, Mayo Foundation, Rochester, MN, 1994.